SCR of NOx in loop reactors: Asymptotic model and bifurcational analysis

This is an electronic version (author's version) of the paper:

Fissore D., Penciu O. M., Barresi A. A. (2006). SCR of NOx in loop reactors: asymptotic models and bifurcational analysis. Chemical Engineering Journal (Elsevier), 122(3), 175-182. DOI: 10.1016/j.cej.2006.05.017.

SCR of NO_x in loop reactors: asymptotic model and bifurcational analysis.

Davide Fissore[*]*, Oana M. Penciu, Antonello A. Barresi*

Dipartimento di Scienza dei Materiali e Ingegneria Chimica,

Politecnico di Torino, corso Duca degli Abruzzi 24,

10129 Torino (Italy)

[*] Author to whom all the correspondence should be addressed, e-mail: davide.fissore@polito.it, tel: +39-(0)11-5644695, fax: +39-(0)11-5644699.

Abstract

The aim of this work is to investigate the Selective Catalytic Reduction (SCR) of NO_x with NH_3 in a loop reactor, which extend the flow-reversal concept to rotating port feeding in a loop-shape system made of *N* units. A simplified model is given and the predictions of this asymptotic model are compared with the results of numerical simulations of a finite-unite reactor model with various number of sections, thus proving the convergence to the asymptotic model. The influence of the main parameters, namely inlet temperature and flow rate, and of the catalyst kinetic parameters is addressed by means of bifurcational analysis.

Keywords

Loop reactors, Chromatographic reactors, Asymptotic models, Selective Catalytic Reduction, Bifurcational Analysis.

Introduction

In many chemical processes, the chemical reaction itself is only one of the several processes taking place. There are often separation and heat exchange processes which are of straightforward importance for the reactor performance and for the following processing steps. In view of this complex picture, reaction engineering is shifting from conventional reactors operating under steady-state to multifunctional and/or transient reactors. This new type of reactors takes advantage of the coupling of several operations into a single equipment, and/or the transient behaviour of them, to improve characteristics such as yield, productivity, flexibility, safety, and investment and operation costs.

Among these multifunctional reactors, the chromatographic reactor, which couples chemical reaction and adsorptive separation, has received a great deal of attention since 1960 as the continuous separation of products can drive a reversible reaction to near completion since it suppresses the rate of the reverse reaction and, at the same time, high purity products are obtained. Chromatographic separations can be achieved in the reverse-flow reactor (RFR) if the reactor is packed with an adsorbent, or with a mixture of adsorbent and catalyst, which has a high adsorption capacity toward a reactant, and low toward a product, so that the periodic switching of the feed traps the strongly adsorbed reactant inside the reactor. Moreover, it can allow trapping the moving heat wave inside the catalytic bed when exothermic reactions take place, thus giving the possibility of exploiting the thermal storage capacity of the catalytic bed, which acts as a regenerative heat exchanger, allowing auto-thermal operation when the adiabatic temperature rise of the feed is low (see, for example, the reviews of Matros & Bunimovich (1996) and Kolios, Frauhammer & Eigenberger (2000)).

The Selective Catalytic Reduction (SCR) of NO_x with ammonia in a RFR using a catalyst that strongly adsorbs the ammonia was firstly suggested by Agar & Ruppel (1988), Noskov et al. (1996) and Synder & Subramaniam (1998): in all these papers

isothermal operation was investigated in order to focus on the interaction between adsorption and chemical reaction, thus neglecting the dynamics of the heat wave. Fissore et al. (2006a) and Botar-Jid et al. (2005) pointed out that even if the adiabatic rise in NO_x removal is usually of the order of 10-20 K, the temperature rise in a RFR will result in a multiple of this value, thus allowing autothermal operation when low temperature gas is fed to the reactor.

Nevertheless the RFR exhibits the problem of wash out, i.e. the emission of unconverted reactants occurring when the flow direction is reversed. Noskov et al. (1996) and Yeong & Luss (2003) proposed various solutions to avoid wash out of unconverted ammonia. Fissore et al. (2006a) studied an alternative reactor configuration to avoid the occurrence of wash out, namely a Loop Reactor made of two or three reactors connected in a closed sequence: a set of valves enables to change the feed position, thus simulating the behaviour of a moving bed and achieving a sustained dynamic behaviour. Contrary to the RFR, the flow direction is maintained in this way, ensuring uniform catalyst exploitation and avoiding wash out. The loop reactor concept was applied by Brinkmann et al. (1999) and by Fissore & Barresi (2003) to the catalytic combustion of lean VOC mixtures, by Velardi & Barresi (2002) to low pressure methanol synthesis and by Fissore, Barresi & Baldi (2003) to synthesis gas production. In all these papers a compact approach was proposed and all the N units are used at all times: in the first interval the reactants are fed through unit 1, whereas the products exit at the end of unit N; in the second interval the reactants are fed through unit 2, whereas the products exit at the end of unit 1; and so on (see Figure 1). The feed and the exit streams are adjacent in this configuration. Sheintuch & Nekhamkina (2005) proposed a different configuration where only N-1 units are used at every time: in the first interval the reactants are fed through unit 1 and the products exit from unit N-1; in the second interval the flow enters at unit 2 and exits from unit N, and so on. This approach requires fewer valves and tubes, but at the cost of a less-efficient use of the catalyst.

In order to properly design and control these periodically forced reactors, it is

necessary to accurately describe all the regime conditions when relevant design and operation parameters are changed. Detailed models, based on the heat and mass balance equations, are usually proposed to investigate the behaviour of these reactors and the properties of the emerging solutions. The most comprehensive approach to accurately describe changes in stability and nature of the regime solutions is the application of bifurcation analysis and of continuation techniques. This approach would be able to characterise all the periodic regimes of these reactors including non-stable regimes such as saddle type and limit cycles (see for example Doedel 1991a, 1991b; Kuznetsov 1998). The main difficulties of this approach both for the RFR and for the loop reactor are the non-autonomous nature of the models and the presence of a discontinuous forcing. In fact standard and popular codes for automatic continuation, such as for example AUTO (Doedel et al., 1997) and CONTENT (Kuznetsov et al., 1996) can be easily applied only to autonomous systems. Russo et al. (2004) pointed out that the spatiotemporal symmetry induced in the system by a cyclic switching of the feed and discharge positions implies that the Poincaré map is the iterate of another non-stroboscopic map and they used this feature to characterize the symmetry of the regime solutions and to carry out bifurcation analysis. Anyway, the application of these techniques to systems with distributed parameters is still a matter of study.

Asymptotic models have been proposed in literature in order to avoid time consuming calculations, not only for bifurcational analysis but also for control purposes. The analogy between the RFR operated with high switching frequency and the countercurrent reactor is well stated (Nieken et al. 1995) and it was exploited, among the others, by Edouard et al. (2005) and by Fissore et al. (2006b) for the design of model based control systems. Sheintuch & Nekhamkina (2005) proposed two limiting pseudo-homogeneous models for a loop reactor with an infinite number of units: the first one is corresponding to an arbitrary switching velocity, while the second corresponds to high switching frequency; they used a pseudo-homogeneous model to describe the loop reactor and a first order exothermic reaction.

The aim of this paper is to develop the asymptotic model for a loop reactor, operated at high switching frequency, where the SCR of NO_x with NH_3 takes place. The structure of the paper is the following: in the next section the mathematical model will be formulated and the asymptote corresponding to the case of fast switching is introduced (FSA). The study of the fast switching asymptote is motivated by the paper by Fissore et al. (2006a) where it was pointed out that high switching frequency was required in the loop reactor in order to achieve and maintain autothermal operation when feeding low temperature reactants. In the third section the predictions of the asymptotic model are compared with the results of numerical simulations of a finite-unit reactor model with various numbers of sections and convergence to the asymptotic model is demonstrated. In the fourth section the bifurcational analysis is used to point out the influence of the main operating variables.

The model

A heterogeneous mathematical model was used to investigate the performance of the loop rector. An Eley-Rideal mechanism is used to describe the reaction between NO_x (A) in the gas phase and the ammonia (B) adsorbed on the catalyst:

$$A + B_S \rightarrow C \tag{1}$$

$$B + S \rightleftarrows B_S \tag{2}$$

The reduction reaction is generally considered to be of first order with respect to each reactant (Tronconi et al., 1996):

$$r_{red} = -k_{red} C_{A,i} \theta_B \Omega \tag{3}$$

where θ_B is the ammonia surface coverage, Ω is the total catalyst capacity and $C_{A,i}$ is the concentration of reactant A at the gas-solid interface. In some papers (Lietti et al., 1998; Nova et al., 2001) the rate of reduction appeared to be essentially independent of the ammonia surface coverage above a critical NH_3 surface concentration (θ_B^v):

$$r_{red} = -k_{red} C_{A,i} \theta_B^{\upsilon} \left(1 - e^{\theta_B / \theta_B^{\upsilon}} \right) \Omega \quad (4)$$

The adsorption rate of ammonia on the catalyst surface is assumed to be proportional to the ammonia concentration in the gas phase and to the free fraction of surface sites:

$$r_{ads} = k_{ads} C_{B,i} \left(1 - \theta_B \right) \Omega \quad (5)$$

while the rate of desorption is assumed to be proportional to the concentration of the adsorbed specie:

$$r_{des} = k_{des} \theta_B \Omega \quad (6)$$

A Temkin-type desorption kinetics, where the activation energy for desorption is a function of the surface coverage, is generally assumed:

$$E_{a,des} = E'_{a,des} \left(1 - \beta \theta_B^{\sigma} \right) \quad (7)$$

An Arrhenius type dependence of the kinetic constants k_{red}, k_{ads} and k_{des} from the temperature is stated:

$$k_{red} = k_{0,red} e^{-\frac{E_{a,red}}{RT_S}}, \; k_{ads} = k_{0,ads} e^{-\frac{E_{a,ads}}{RT_S}}, \; k_{des} = k_{0,des} e^{-\frac{E_{a,des}}{RT_S}} \quad (8)$$

Table 1 gives some values of the kinetic parameters of the adsorption/reduction/desorption reactions that can be found in the literature.

The SCR reaction is assumed to take place in a monolith: mass and energy dispersive transport are not taken into account, due to the low conductivity of the monolithic support, and also pressure loss inside the reactor is neglected; adiabatic operation is assumed. Thus, if the rate of reduction is supposed to be independent of the ammonia surface coverage (i.e. eq. (3) holds) the system of partial differential equations that describes the process dynamics is the following:

- gas phase mass balance:

$$\frac{\partial C_A^*}{\partial t^*} = -v^* \frac{\partial C_A^*}{\partial x^*} + Pe_A \left(C_{A,i}^* - C_A^* \right) \quad (9)$$

$$\frac{\partial C_B^*}{\partial t^*} = -v^* \frac{\partial C_B^*}{\partial x^*} + Pe_B \left(C_{B,i}^* - C_B^* \right) \quad (10)$$

- solid phase mass balance:

$$\frac{\partial \theta_B}{\partial t^*} = Da_{ads} e^{-\gamma_{ads}\left(\frac{1}{T_S^*}-1\right)} C_{B,i}^* \left(1-\theta_B\right) - Da_{des} e^{-\gamma_{des}\left(\frac{1}{T_S^*}-1\right)} e^{\gamma_{des}\frac{\beta\theta_B^\sigma}{T_S^*}} \theta_B - Da_{red} e^{-\gamma_{red}\left(\frac{1}{T_S^*}-1\right)} C_{A.i}^* \theta_B \tag{11}$$

- gas phase energy balance:

$$\frac{\partial T_G^*}{\partial t^*} = -v^* \frac{\partial T_G^*}{\partial x^*} - St\left(T_G^* - T_S^*\right) \tag{12}$$

- solid phase energy balance:

$$\begin{aligned} \alpha \frac{\partial T_S^*}{\partial t^*} = St\left(T_G^* - T_S^*\right) + Da_{red} \frac{\Delta T_{ad,red}}{T_{G,0}} C_{A.i}^* \theta_B e^{-\gamma_{red}\left(\frac{1}{T_S^*}-1\right)} A + \\ Da_{ads} \frac{\Delta T_{ad,ads}}{T_{G,0}} C_{B,i}^* \left(1-\theta_B\right) e^{-\gamma_{ads}\left(\frac{1}{T_S^*}-1\right)} A - Da_{des} \frac{\Delta T_{ad,des}}{T_{G,0}} \theta_B e^{-\gamma_{des}\left(\frac{1}{T_S^*}-1\right)} e^{\gamma_{des}\frac{\beta\theta_B^\sigma}{T_S^*}} A \end{aligned} \tag{13}$$

where the non-dimensional parameters, obtained dividing by quantity evaluated at inlet conditions, are defined as follows:

$$x^* = \frac{x}{L},\ v^* = \frac{v_G}{v_{G,0}},\ t^* = t\frac{v_{G,0}}{L},\ \alpha = \frac{\varepsilon\rho_S c_{p,S}}{\rho_G c_{p,G}}, A = \frac{\Omega}{C_{A,0}},$$

$$C_A^* = \frac{C_A}{C_{A,0}},\ C_{A,i}^* = \frac{C_{A.i}}{C_{A,0}},\ C_B^* = \frac{C_B}{C_{A,0}},\ C_{B,i}^* = \frac{C_{B.i}}{C_{A,0}},\ T_G^* = \frac{T_G}{T_{G,0}},\ T_S^* = \frac{T_S}{T_{G,0}},$$

$$Pe_A = \frac{h_A a_v L}{v_{G,0}},\ Pe_B = \frac{h_B a_v L}{v_{G,0}},\ St = \frac{h_T a_v L}{\rho_G c_{P,G} v_{G,0}},$$

$$\gamma_{ads} = \frac{E_{a,ads}}{RT_{G,0}},\ \gamma_{des} = \frac{E'_{a,des}}{RT_{G,0}},\ \gamma_{red} = \frac{E_{a,red}}{RT_{G,0}},$$

$$Da_{ads} = \frac{k_{0,ads} e^{-\gamma_{ads}} L C_{A,0}}{v_{G,0}},\ Da_{des} = \frac{k_{0,des} e^{-\gamma_{ads}} L}{v_{G,0}},\ Da_{red} = \frac{k_{0,red} e^{-\gamma_{red}} L}{v_{G,0}},$$

$$\Delta T_{ad,ads} = \frac{(-\Delta H_{ads}) C_{A,0}}{\rho_G c_{p,G}},\ \Delta T_{ad,des} = \frac{(-\Delta H_{des}) C_{A,0}}{\rho_G c_{p,G}},\ \Delta T_{ad,red} = \frac{(-\Delta H_{red}) C_{A,0}}{\rho_G c_{p,G}}.$$

Non-dimensional parameters are used so that the obtained results are of general validity, i.e. the same results can be obtained proven that the non-dimensional parameters of the systems have the same value. The values of $C_{A,i}$ and $C_{B,i}$, i.e. the gas concentration at the interface, are calculated from the mass balance at the gas-solid interface, assuming that there is no accumulation, i.e.:

$$-Pe_A\left(C^*_{A,i}-C^*_A\right)=Da_{red}e^{-\gamma_{red}\left(\frac{1}{T^*_S}-1\right)}C^*_{A.i}\theta_B\Omega \tag{14}$$

$$Pe_B\left(C^*_{B,i}-C^*_B\right)=Da_{ads}e^{-\gamma_{ads}\left(\frac{1}{T^*_S}-1\right)}C^*_{B,i}\left(1-\theta_B\right)\Omega-Da_{des}e^{-\gamma_{des}\left(\frac{1}{T^*_S}-1\right)}e^{\gamma_{des}\frac{\beta\theta^\sigma_B}{T^*_S}}\theta_B\Omega \tag{15}$$

The concentration of each reactant in the feed is the same while the rest is inert gas. The catalyst is pre-heated to a uniform temperature of 600 K; as a consequence the initial conditions are:

$$\begin{aligned}
&C^*_A\left(x^*\right)=0 \quad x^*\in[0,1], t=0\\
&C^*_B\left(x^*\right)=0 \quad x^*\in[0,1], t=0\\
&\theta_B\left(x^*\right)=0 \quad x^*\in[0,1], t=0\\
&T^*_G\left(x^*\right)=\frac{T_{ph}}{T_{G,0}} \quad x^*\in[0,1], t=0\\
&T^*_S\left(x^*\right)=\frac{T_{ph}}{T_{G,0}} \quad x^*\in[0,1], t=0
\end{aligned} \tag{16}$$

while the boundary conditions are:

$$\begin{aligned}
&C^*_A=1 \quad x^*=0, t\geq 0\\
&C^*_B=1 \quad x^*=0, t\geq 0\\
&T^*_G=1 \quad x^*=0, t\geq 0
\end{aligned} \tag{17}$$

the other operating conditions are given in Table 2 and in the captions of the Figures.

The system of partial differential equations (9) - (13) is solved by discretising the domain of the spatial variables into a grid of 60 points, equally spaced, thus obtaining a grid-independent solution; an upwind discretisation scheme has been used. The MatLAB solver ode15s, which is a quasi-constant implementation of the Numerical Differentiation Formulas in terms of Backward Differences (Shampine & Reichelt, 1997) is used to solve the system; the relative and absolute tolerances are set equal to the square root of the working machine precision. After a transient period, the solution of the system evolves towards a periodic-steady state (PSS): the behaviour of the reactor (temperature and concentration profiles) is the same within every cycle.

Fast Switching Asymptote

Following the approach by Sheintuch and Nekhamkina (2005), a loop reactor of N identical units, each one of the length $\Delta L=L/N$ is considered, and the inlet/outlet ports are switched at every time interval t_c. The boundary conditions are thus applied at positions that vary in time as stepwise functions with a total period $\lambda=N\cdot t_c$:

$$x_{in}^{*}=(n-1)\cdot\Delta L \text{ when } t\in\left[(n-1)t_c+k\lambda, nt_c+k\lambda\right] \qquad n=1,...,N \quad k=0,1,... \tag{18}$$

where n identifies the number of the reactor of the loop and k the cycle. The outlet position almost coincides with the inlet.

To simplify the analysis of the most important parameters it is considered the limiting case of the fast switching asymptote when the switching velocity v_{sw} defined as:

$$v_{sw}=\frac{\Delta L}{t_c}=\frac{L}{N\cdot t_c} \tag{19}$$

is considered to be significantly faster than the gas velocity and the period λ is assumed to be smaller than all other characteristic time scales, namely the characteristic time for convection, adsorption, desorption and reduction reaction. So, it is possible to define the switching cycle-averaged variables $\overline{C_A^*}(t^*,x^*)$, $\overline{C_B^*}(t^*,x^*)$, $\overline{T_G^*}(t^*,x^*)$ and in the limit of many ports and fast switching the axial profiles of C_A^*, C_B^*, T_G^* are continuous.

Let us consider the enthalpy balance during the time interval $t_f \gg \lambda$ for a control volume of the length $\Delta L=L/N$ which combines two halves of adjacent sections (see Figure 2):

$$\left\{T_G\left(t+t_f\right)-T_G\left(t\right)\right\}\rho_G c_{p,G} S\Delta L=\left\{q_1-q_2+q_{in}-q_{out}-q_{ex}\right\}t_f \tag{20}$$

where:

- q_1 and q_2 are the heat flows entering and exiting from the volume $S\Delta L$ by convection:

$$q_1-q_2=v_G\rho_G S c_{p,G}\left(T_{G,1}-T_{G,2}\right) \tag{21}$$

- q_{in} and q_{out} are the heat flow of the feed and of the product extracted from the

reactor:

$$q_{in} - q_{out} = v_G \rho_S S c_{p,G} \left(T_{G,0} - T_G \right) \qquad if \quad 0 < t < t_c \tag{22}$$

otherwise this term is equal to zero because the intermediate part of the control volume acts as the inlet/outlet only during the short time interval t_c;

- q_{ex} is the heat flow exchanged with the solid:

$$q_{ex} = h_T a_v S \Delta L \left(T_G - T_S \right) \tag{23}$$

The resulting heat balance is made non-dimensional by means of the quantities previously defined and, in the limit $\lambda \to 0$ and $\Delta L \to 0$ the energy balance for the gas phase takes the form:

$$\frac{\partial \overline{T_G^*}}{\partial t^*} = -v^* \frac{\partial \overline{T_G^*}}{\partial x^*} - St(\overline{T_G^*} - \overline{T_S^*}) - v^*(\overline{T_G^*} - T_{G,0}^*) \tag{24}$$

Similarly, this procedure can be applied also to the mass balance of NO_x and NH_3 for the same control volume, thus leading to the equations:

$$\frac{\partial \overline{C_A^*}}{\partial t^*} = -v^* \frac{\partial \overline{C_A^*}}{\partial x^*} + Pe_A \left(C_{A,i}^* - \overline{C_A^*} \right) - v^* \left(\overline{C_A^*} - 1 \right) \tag{25}$$

$$\frac{\partial \overline{C_B^*}}{\partial t^*} = -v^* \frac{\partial \overline{C_B^*}}{\partial x^*} + Pe_B \left(C_{B,i}^* - \overline{C_B^*} \right) - v^* \left(\overline{C_B^*} - \frac{C_{B,0}}{C_{A,0}} \right) \tag{26}$$

The last terms in eq. (24)-(26) shows that the discrete supply/removal acting at each port of a finite unit system during a short interval is incorporated into the limiting continuous model as permanently acting distributed source/sink terms.

The heat and mass balance equations for the solid can be written for the same control volume and are not changed with respect to eq. (11) and (13); obviously the value of the temperature is substituted by the integral mean.

Results

Performance of the FSA model

The results confirm that in order to be allowed to use the FSA it is compulsory to verify that:

1) the switching velocity is much faster than the gas velocity,

2) the period $\lambda = Nt_c$ is smaller than all other characteristic time scales.

As concerns the first point, $v_{sw} \gg v_G$ implies that:

$$t_c \ll \frac{T_{G,0}}{T_G}\frac{L}{N}\frac{1}{v_{G,0}} \tag{27}$$

This means that, in order to use the simplified model, the switching time should be decreased when the total reactor length or the inlet gas temperature are decreased as well as when the number of reactors and the inlet flow rate are increased. Thus, for a fixed value of the gas flow rate (and thus of the gas velocity) and of the number of reactors, the lower is the switching time the better is the approximation obtained. Figure 3 shows that for a certain configuration of the network, in this case made up of three reactors, when the switching time is reduced the temperature and concentration axial profiles converges to a limiting curve which is that predicted by the FSA (the solid temperature profiles is shown in the upper graph, while the NO_x concentration is shown in the lower graph).

The second point requires that the period $\lambda = Nt_c$ is smaller than all other characteristic time scales, namely the characteristic time for convection, adsorption, desorption and reduction reaction which are a function of the catalyst used (and can be calculated once the kinetic parameters of the catalyst are known).

Bifurcational analysis

If the two previously stated conditions are fulfilled, this simplified model can be used for the bifurcational analysis. At first isothermal operation has been considered: this assumption allows simplifying the analysis, enabling to focus on the impact of the operating conditions on the dynamic features caused by the trapping of one reactant in the reactor; the model is thus made up of eq.(25)-(26) and eq. (11). Figures 4-6 show the results obtained by means of bifurcational analysis when the bifurcational parameter is Da_{red}, Da_{ads} and Da_{des} respectively. The aim of this study is to point out the role played by catalyst activity on the results obtained in the loop

reactor, thus giving general guidelines for catalyst design. Results are given in terms of

$$C_M^* = C_A^* + \xi C_B^* \tag{28}$$

This because environmental regulations may limit the release of both species. In various applications, such as the destruction of NO_x by NH_3, ξ can be larger than unity. With this assumption, our results are absolutely general and their validity is not restricted to the SCR process only, proven that the non-dimensional parameters are calculated for the process under investigation.

Figure 4 shows, for example, that an enhancement of the adsorptive capacity of the catalyst (Da_{ads}) has a stronger impact on the reaction yield than an increase of the catalytic activity (Da_{red}); this conclusion is confirmed also when the value of the penalty factor ξ is changed (lower graph) . The role played by the adsorption process is much more important when the catalytic activity is high, as it is pointed out in Figure 5 (upper graph) where, in presence of the same increase of Da_{ads}, the outlet reactants concentration decreases much more when Da_{red} is high. Similarly, desorption kinetic parameters can have a stronger influence on reactors performance than the reduction kinetic parameters as it is pointed out in Figure 5 (lower graph). This analysis can be used for the design of the catalyst that has to be used in this process: higher values of Da_{ads} means that the catalyst should have a high number of sites where ammonia can adsorb, while Da_{red} and Da_{des} can be controlled by modifying the type and strength of the NH_3-NO_x bond. Few minutes are generally required to get charts like those of Figure 4-5 which can be used to find out the optimal characteristics of the catalyst as a function of the process considered.

Beside this type of study, bifurcational analysis can be obviously used to find out the operating conditions that allow satisfying the operation goals. As far as non-isothermal operation is concerned, bifurcational analysis can be used to evaluate the inlet gas temperature that allows for autothermal operation. Figure 6 (upper graph) shows the results that are obtained using the kinetic parameters of the four catalysts given in Table 1. Only if the most active catalyst, the one studied by Tronconi et al.

(1996) is used, autothermal operation can be obtained with a low (ambient) temperature feeding, otherwise the feed should be pre-heated and the non-stationary operation can have no more advantages over the traditional reactors. Figure 6 (lower graph) evidences that the gas velocity should be kept low in order to get autothermal operation in presence of an ambient temperature feeding: in presence of high values of the flow rate, the gas convection can extract the reaction heat from the catalyst, leading the reaction to irreversible extinction. Obviously, the higher the value of the penalty factor, the lower the gas velocity that allows for autothermal behavior. These charts can be used to find out the value of the volume of catalyst that should be used to get autothermal regime with high conversion.

Conclusions

The loop reactor operated with high switching frequency has been investigated in this paper. The SCR of NO_x with NH_3 has been used as a case study as previous studies evidenced that this process can take substantial advantages from this mode of reactor operation. A simplified model has been introduced and the range of operating variables for which this assumption is acceptable has been discussed. The predictions of the asymptotic model have been compared with the results of numerical simulations of a reactor with a finite number of units and the convergence to the asymptotic model is proven.

The influence of the main parameters, namely inlet temperature and flow rate, and of the kinetic parameters of the adsorption, of the desorption and of the reduction reaction on the performance of these devices has been addressed by means of bifurcational analysis using the simplified model, showing how the analysis can be used to find out the operating conditions that allows for an autothermal regime with high conversion.

Acknowledgements

Oana Marlena Penciu is grateful to the European Commission for a Marie Curie Training Site Fellowship that supported her during a stage at Politecnico di Torino (SICOFOR, Contract Nr. HPMT-CT-2001-00343). The authors would like to thank Prof. Moshe Sheintuch and Olga Nekhamkina for their valuable suggestions in the development of the simplified model.

Notation

A	non-dimensional catalyst capacity
a_v	specific surface of the catalyst, $m^2\ m^{-3}$
C	gas phase concentration, $mol\ m^{-3}$
c_p	specific heat, $J\ kg^{-1}\ K^{-1}$
Da	Damköhler number
E_a	activation energy, $J\ mol^{-1}$
$E'_{a,des}$	activation energy of the desorption reaction at zero coverage, $J\ mol^{-1}$
h_i	mass transfer coefficient for the i-th species, $m\ s^{-1}$
h_T	heat transfer coefficient, $J\ m^{-2}\ s^{-1}\ K^{-1}$
$-\Delta H$	heat of reaction, $J\ mol^{-1}$
L	total reactor length, m
ΔL	length of each reactor of the loop, m
k	number of cycles
k_{ads}	adsorption rate constant, $m^3\ mol^{-1}\ s^{-1}$
k_{des}	desorption rate constant, s^{-1}
k_{red}	reduction rate constant, $m^3\ mol^{-1}\ s^{-1}$
$k_{0,ads}$	frequency factor of the adsorption rate constant, $m^3\ mol^{-1}\ s^{-1}$
$k_{0,des}$	frequency factor of the desorption rate constant, s^{-1}
$k_{0,red}$	frequency factor of the reduction rate constant, $m^3\ mol^{-1}\ s^{-1}$
n	number of the reactor in the loop
N	total number of reactors in the loop
Pe	Peclet number
q_{ex}	heat flow exchanged with the solid, $J\ s^{-1}$
q_{in} (q_{out})	heat flow of the feed (product) stream, $J\ s^{-1}$
q_1 (q_2)	heat flow entering (exiting) from the volume $S\Delta L$ by convection, $J\ s^{-1}$

r	rate of reaction, mol s^{-1} m^{-3}
R	ideal gas constant, J K^{-1} mol^{-1}
S	cross section area, m^2
St	Stanton number
t	time, s
t_c	switching time, s
t_f	time interval, s
T	temperature, K
ΔT_{ad}	non-dimensional adiabatic temperature rise
v	gas velocity, m s^{-1}
v_{sw}	switching velocity, m s^{-1}
x	spatial coordinate, m

Greeks

α	ratio between the solid and the gas heat capacity
β, σ	parameters for the surface coverage dependence of $E_{a,des}$
γ	non-dimensional activation energy
ε	monolith void fraction
θ	surface coverage
θ_B^v	critical NH_3 surface coverage
λ	period of the operation, s
ρ	density, kg m^{-3}
ξ	penalty factor
Ω	catalyst capacity, mol m^{-3}

Subscripts and Superscripts

(overlay)	average over a time interval larger than the period λ

0	feeding condition
A, B	reactants
ads	adsorption reaction
des	desorption reaction
G	gas phase
i	gas-solid interface value
in	inlet position
M	weighted reactants concentration
ph	pre-heating value
red	reduction reaction
S	solid phase
*	non-dimensional value

Abbreviations

FSA	Fast Switching Asymptote
PSS	Periodic Steady-State
RFR	Reverse Flow Reactor
RN	Reactors Network
SCR	Selective Catalytic Reduction

References

Agar, D. W., & Ruppel, W. (1988). Extended reactor concept for dynamic DeNOx design. *Chemical Engineering Science*, 43, 2073-2078.

Brinkmann, M., Barresi, A. A., Vanni, M., & Baldi, G. (1999). Unsteady-state treatment of very lean waste gases in a network of catalytic burners. *Catalysis Today*, 47, 263-277.

Botar-Jid, C. C., Agachi, P. S., Fissore, D., & Barresi, A. A. (2005). Selective Catalytic reduction of NO_x with NH_3 in unsteady-state reactors. *Studia Universitatis Babes-Bolyai. Chemia*, 50 (special Issue for CAPE Forum 2005), 29-40.

Doedel, E. J., Keller, H. B., & Kernevez, J. P. (1991a). Numerical analysis and control of bifurcation problems, Part I. *International Journal of Bifurcation and Chaos in Applied Sciences and Engineering*, 1, 493-520.

Doedel, E. J., Keller, H. B., & Kernevez, J. P. (1991b). Numerical analysis and control of bifurcation problems, Part II. *International Journal of Bifurcation and Chaos in Applied Sciences and Engineering*, 1, 745-772.

Doedel, E. J., Champneys, A. R., Fairgrieve, T. F., Kuznetsov, Y. A., Sanstede, B., & Wang, X. (1997). AUTO97: continuation and birfurcation software for ordinary differential equations. Available by ftp from ftp:cs:concordia:ca in directory Pub/doedel/auto, Department of Computer Science, Concordia University, Montreal, Canada.

Edouard, D., Dufour, P., & Hammouri, H. (2005). Observer based multivariable control of a catalytic reverse flow reactor: Comparison between LQR and MPC approaches. *Computers Chemical Engineering*, 29, 851-865.

Fissore, D., & Barresi, A. A. (2002). Comparison between the reverse-flow reactor and a network of reactors for the oxidation of lean VOC mixtures, *Chemical Engineering Technology*, 25, 421-426.

Fissore, D., Barresi, A. A., & Baldi, G. (2003). Synthesis gas production in a forced unsteady state reactor network. *Industrial & Engineering Chemistry Research*, 42,

2489-2495.

Fissore, D., Barresi, A. A., & Botar-Jid, C. C. (2006a). NO_x removal in forced unsteady-state chromatographic reactors. *Chemical Engineering Science*, 61, 3409-3414.

Fissore D., Edouard D., Hammouri H., & Barresi A. A. (2006b). Non-linear soft-sensors design for unsteady-state VOC afterburners. *AIChE Journal*, 52, 282-291.

Kolios, G., Frauhammer, J., & Eigenberger, G. (2000). Authothermal fixed bed reactor concepts. *Chemical Engineering Science*, 55, 5945-5967.

Kuznetsov, Y. A. (1998). Elements of applied bifurcation theory. 2nd ed., Springer Verlag, New York.

Kuznetsov, Y. A., Levitin, V. V., & Skovoroda, A. R. (1996). Continuation of stationary solutions to evolution problems in CONTENT. Report AM-R9611, Centrum voor Wiskunde en Informatica, Amsterdam, The Netherlands.

Lietti, L., Nova, I., Tronconi, E., & Forzatti, P. (1998). Transient kinetic study of the SCR-DeNO$_x$ reaction. *Catalysis Today*, 45, 85-92.

Matros, Y. H., & Bunimovich, G. A. (1996). Reverse flow operation in fixed bed catalytic reactors. *Catalysis Review-Science and Engineering*, 38, 1-68.

Nieken, U., Kolios, G. & Eigenberger, G. (1995). Limiting cases and approximate solutions for fixed-bed reactors with periodic flow reversal. *AIChE Journal*, 41, 1915-1925.

Noskov, A., Bobrova, L., Bunimovich, G., Goldman, O., Zagoriuko A., & Matros, Y. (1996). Application of the non-stationary state of catalyst surface for gas purification from toxic impurities. *Catalysis Today*, *27*, 315-319.

Nova, I., Lietti, L., Tronconi, E., & Forzatti, P. (2001). Transient response method applied to the kinetic analysis of the DeNO$_x$ SCR reaction. *Chemical Engineering Science*, 56, 1229-1237.

Russo, L., Crescitelli, S., Mancusi, E., & Maffettone, P. L. (2004). Nonlinear analysis of a network of three continuous stirred tank reactors with periodic feed switching: Symmetry and symmetry-breaking. *International Journal of Bifurcation and Chaos in Applied Sciences and Engineering*, 14, 1325-1341.

Sheintuch, M., & Nekhamkina, O. (2005). The asymptotes of loop reactors. *AIChE Journal*, 51, 224-234.

Shampine, L. F., & Reichelt, M. W. (1997). The MatLab ode suite. *SIAM Journal on Scientific Computing*, 18, 1-22.

Synder, J. D., & Subramanian, B. (1998). Numerical simulations of a reverse flow NOx-SCR reactor with side-stream ammonia addition. *Chemical Engineering Science*, 53, 727-734.

Tronconi, E., Lietti, L., Forzatti, P., & Malloggi, S. (1996). Experimental and theoretical investigation of the dynamics of the SCR-DeNOx reaction. *Chemical Engineering Science*, 51, 2965-2970.

Yeong, J., & Luss, D. (2003). Pollutant destruction in a reverse-flow chromatographic reactor. *Chemical Engineering Science*, 58, 1095-1102.

Velardi, S. A., & Barresi, A. A. (2002). Methanol synthesis in forced unsteady-state reactor network. *Chemical Engineering Science*, 57, 2995-3004.

List of figures

Table 1 Values of the kinetic parameters used in the simulations.

Model	1	2	3	4
	Tronconi et al. (1996)	Lietti et al. (1998) V_2O_5-WO_3/TiO_2	Lietti et al. (1998) V_2O_5/TiO_2	Nova et al. (2001)
$k_{0,red}$, s^{-1}	$9.8 \cdot 10^9$	$8.39 \cdot 10^5$	$1.08 \cdot 10^6$	$1.18 \cdot 10^8$
$E_{a,red}$, J mol^{-1}	77891	59412.8	66944	80332.8
θ_B^{υ}	-	0.108	0.076	0.06
$k_{0,ads}$, m^3 mol^{-1} s^{-1}	$3.4 \cdot 10^5$	0.614	0.820	33.87
$E_{a,ads}$, J mol^{-1}	37656	0.0	0.0	0.0
$k_{0,des}$, s^{-1}	$4.1 \cdot 10^7$	$1.99 \cdot 10^5$	$3.67 \cdot 10^6$	$2.2 \cdot 10^6$
$E'_{a,des}$, J mol^{-1}	123428	97905.6	107947.2	96232
β	0.315	0.448	0.310	0.256
σ	1.0	1.0	1.0	1.0

Table 2 Values of the main operating parameters used in the simulations.

Ω	210 mol m^{-3}
L	0.45 m
ε	0.65
ρ_S	2500 kg m^{-3}
$c_{p,S}$	0.9 kJ kg^{-1} K^{-1}
ΔH_{red}	-406 kJ mol^{-1}
ΔH_{ads}	-13 kJ mol^{-1}
ΔH_{des}	13 kJ mol^{-1}
$T_{G,0}$	298 K

Figure 1

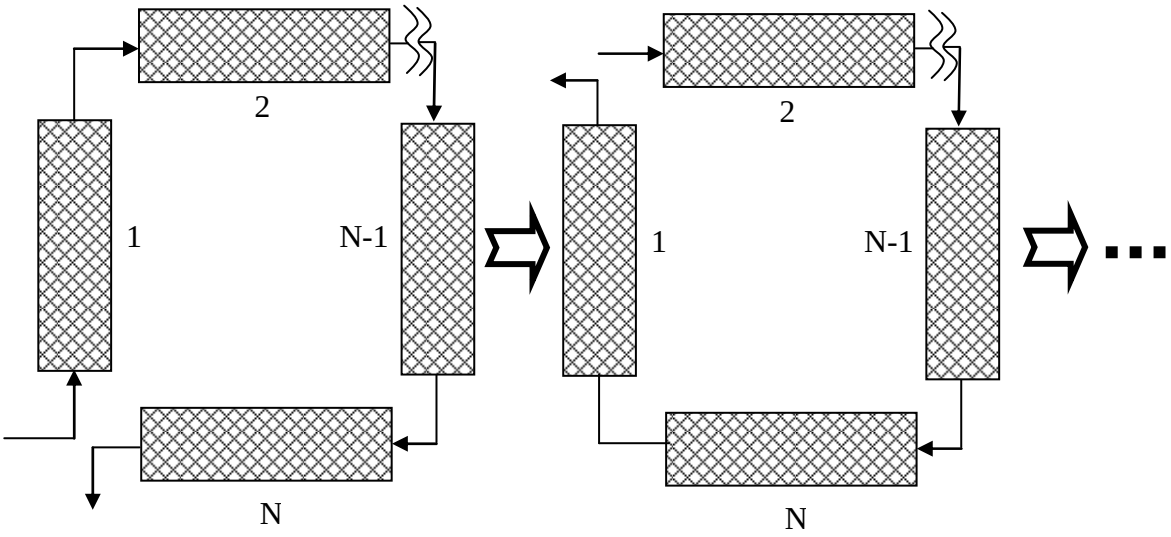

Figure 2

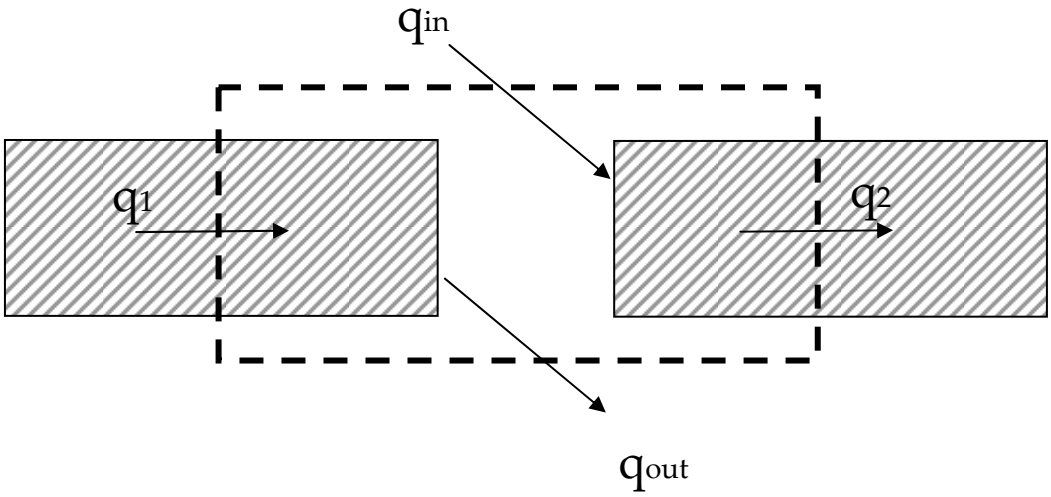

Figure 3

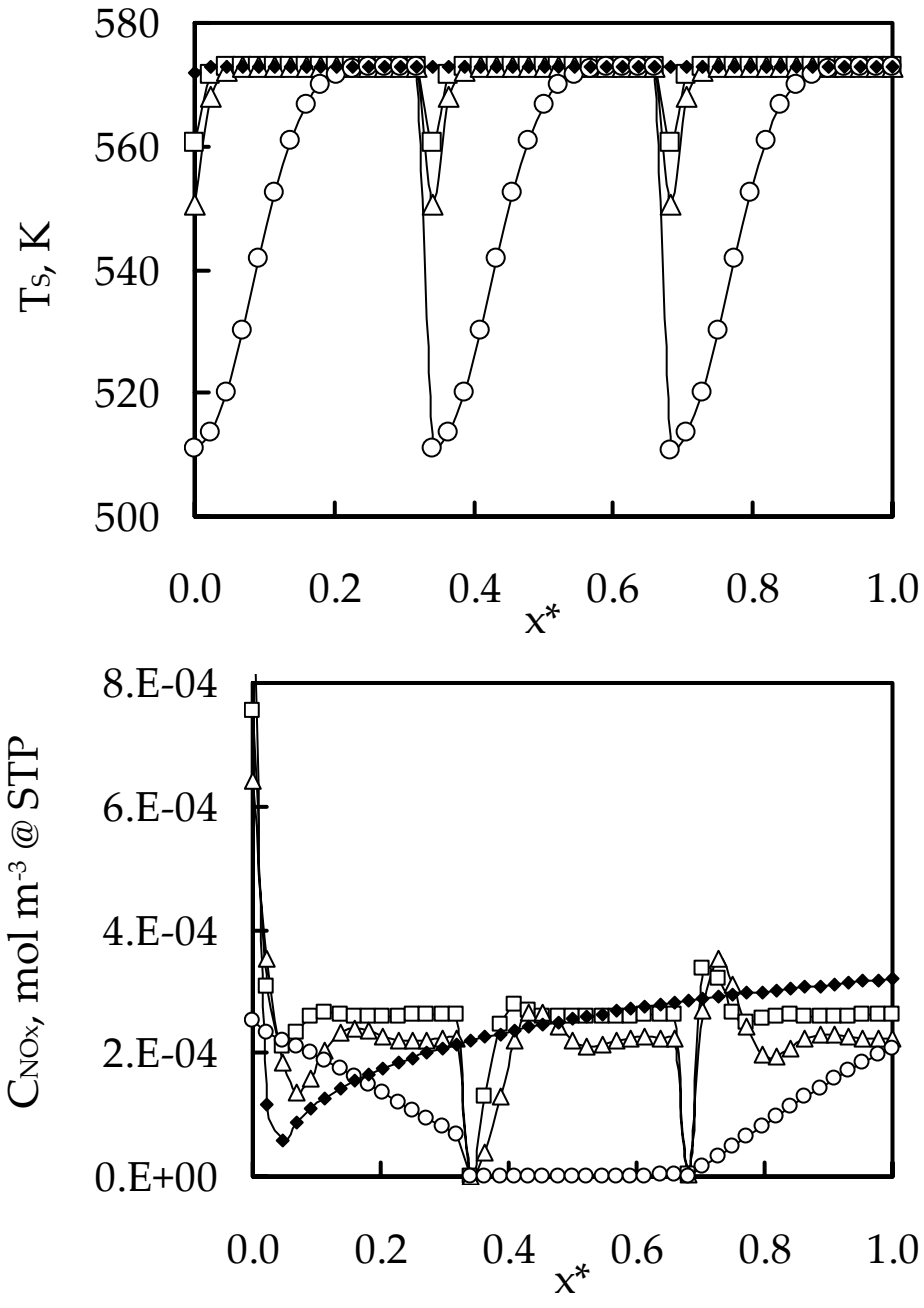
580
560
540
520
500
T_S, K
0.0
0.2
0.4
0.6
0.8
1.0
x*
8.E-04
6.E-04
4.E-04
2.E-04
0.E+00
C_{NOx}, mol m^{-3} @ STP
0.0
0.2
0.4
0.6
0.8
1.0
x*

Figure 4

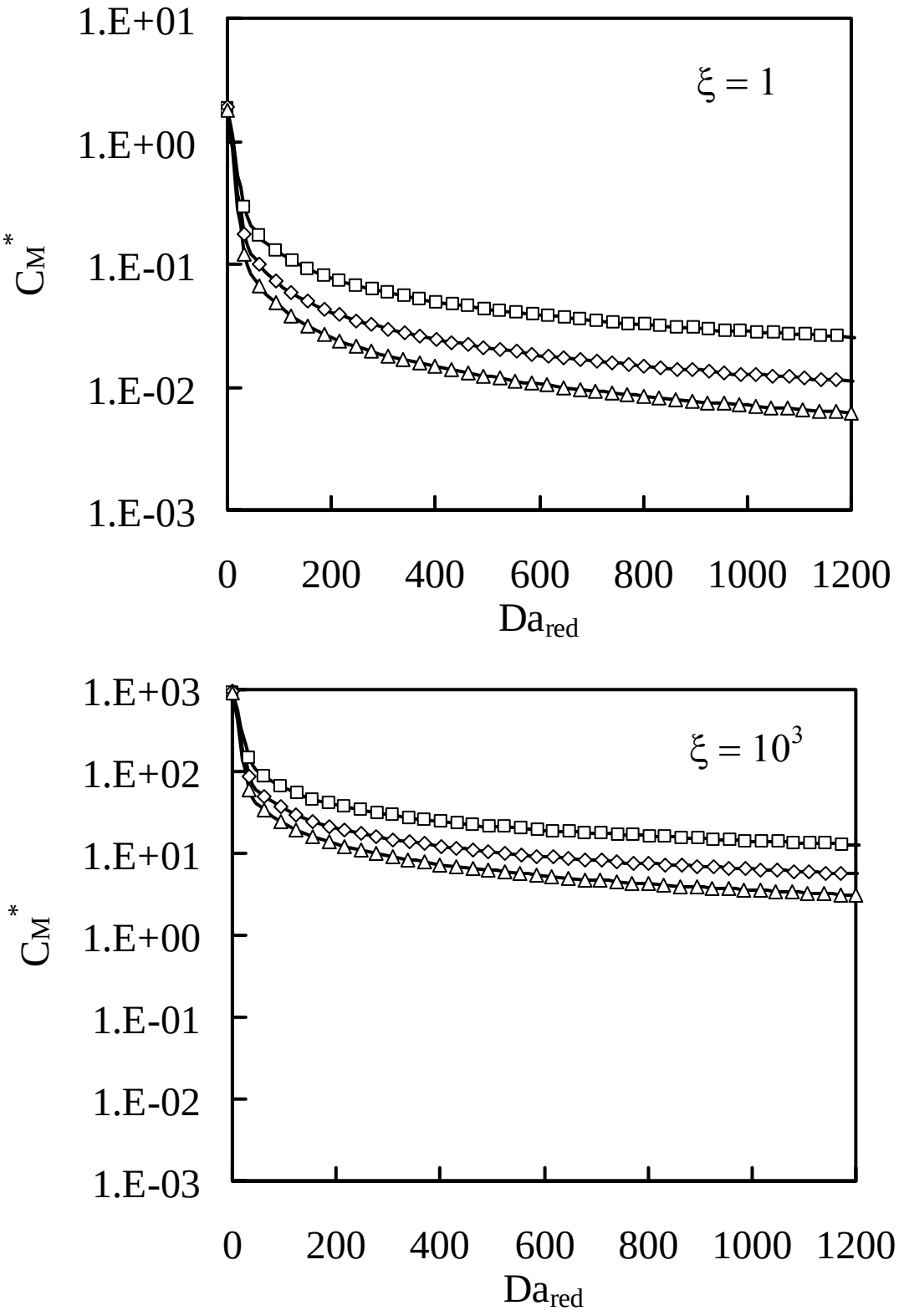
1.E+01
1.E+00
1.E-01
1.E-02
1.E-03
C_M^*
$\xi = 1$
0
200
400
600
800
1000
1200
Da_{red}
1.E+03
1.E+02
1.E+01
1.E+00
1.E-01
1.E-02
1.E-03
C_M^*
$\xi = 10^3$
0
200
400
600
800
1000
1200
Da_{red}

Figure 5

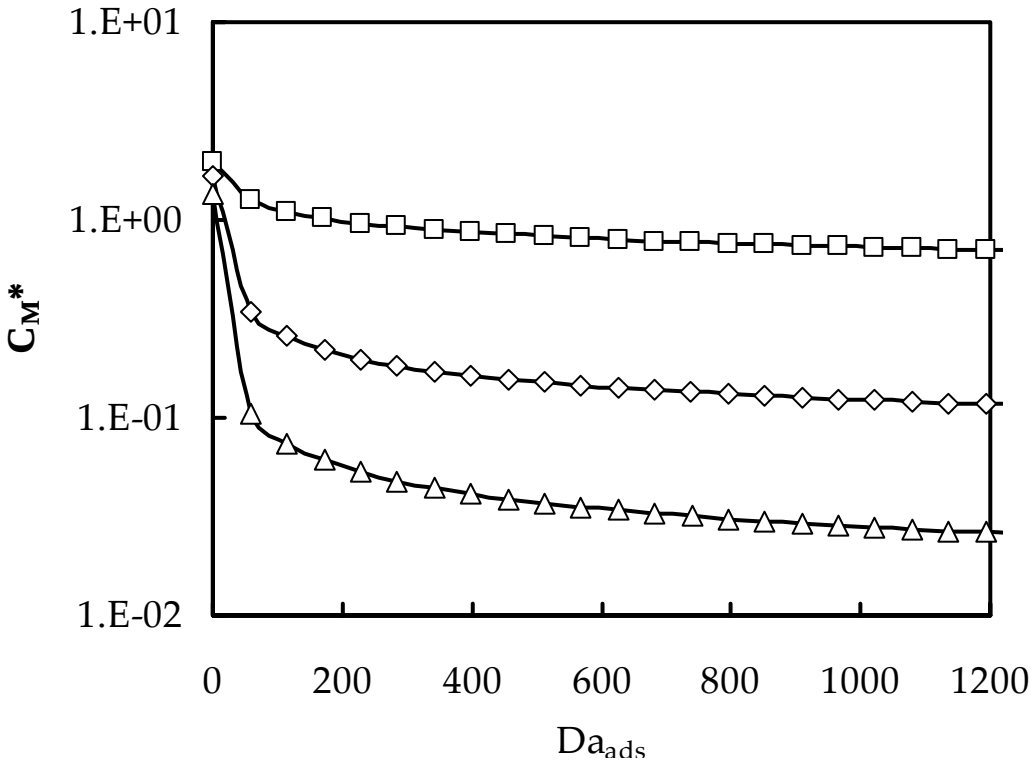
1.E+01
1.E+00
1.E-01
1.E-02
C_M^*
0
200
400
600
800
1000
1200
Da_{ads}

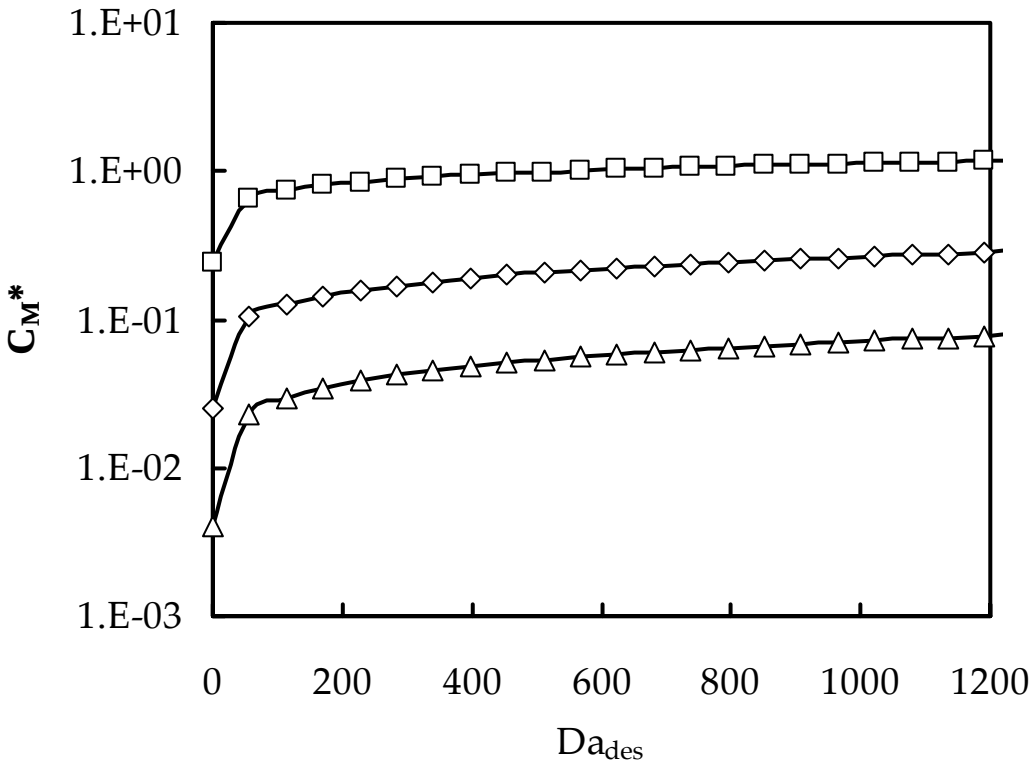
1.E+01
1.E+00
1.E-01
1.E-02
1.E-03
C_M^*
0
200
400
600
800
1000
1200
Da_{des}

Figure 6

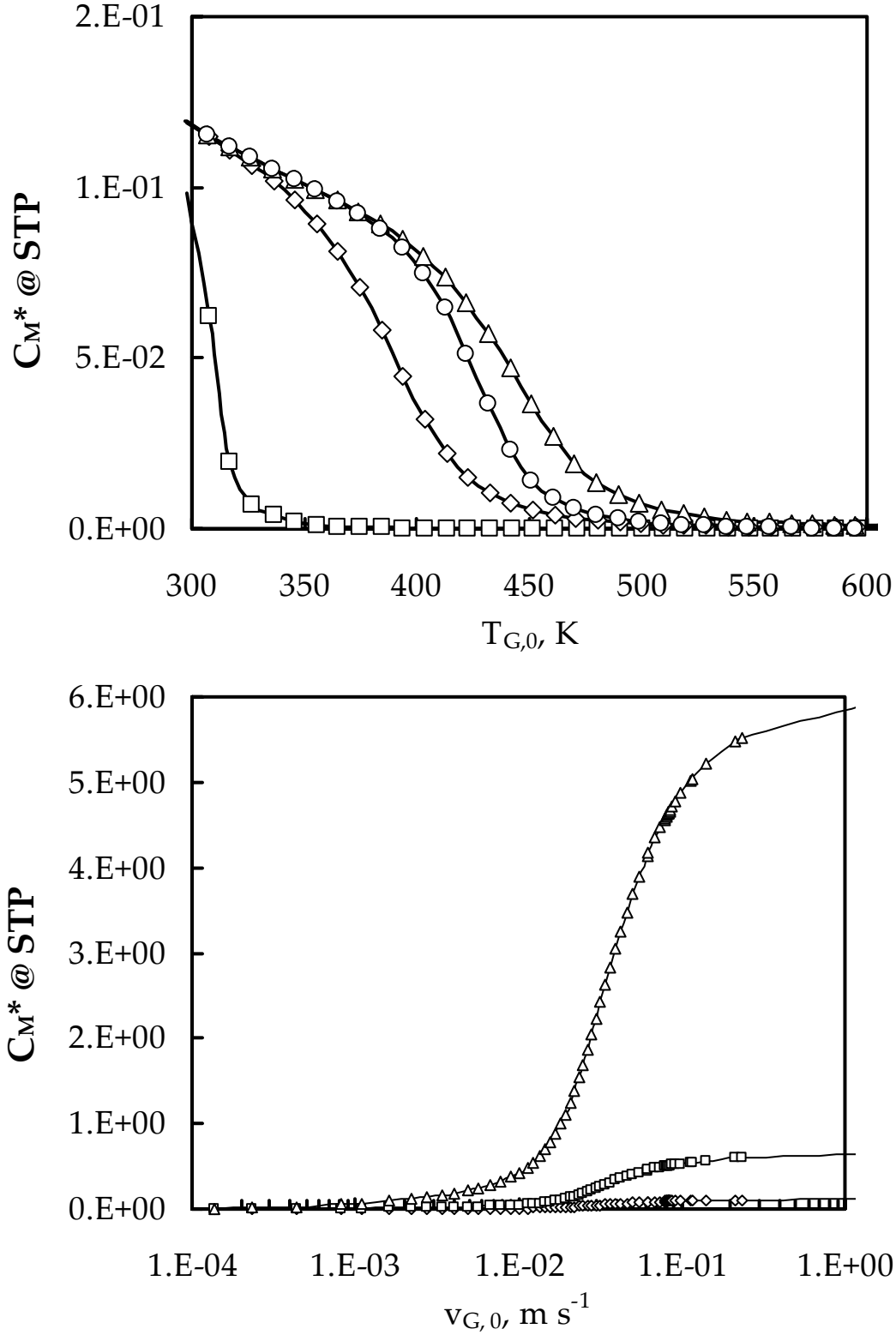
2.E-01
1.E-01
5.E-02
0.E+00
C_M* @ STP
300
350
400
450
500
550
600
$T_{G,0}$, K
6.E+00
5.E+00
4.E+00
3.E+00
2.E+00
1.E+00
0.E+00
C_M* @ STP
1.E-04
1.E-03
1.E-02
1.E-01
1.E+00
$v_{G,0}$, m s^{-1}